

# Many-spin interactions and spin excitations in $\text{Mn}_{12}$

M. I. Katsnelson

*Institute of Metal Physics, Ekaterinburg 620219, Russia*

V. V. Dobrovitski and B. N. Harmon

*Ames Laboratory, Iowa State University, Ames, Iowa 50011*

(Received 13 July 1998)

In this work, the many-spin interactions taking place in  $\text{Mn}_{12}$  large-spin clusters are extensively studied using the 8-spin model Hamiltonian, for which we determine the possible parameters based on experimental data. Account of the many-spin excitations satisfactorily explains positions of the neutron scattering peaks, results of EPR measurements, and the temperature dependence of magnetic susceptibility. In particular, strong Dzyaloshinsky-Morya interactions are found to be important for description of neutron scattering data.

[S0163-1829(99)09809-4]

## INTRODUCTION

In the past years, a new kind of magnetic compounds, the magnetic molecules, has been drawing the attention of physicists as well as chemists.<sup>1</sup> Such molecules each contain a large number (typically, 10 to 20) of paramagnetic ions (such as Mn, Fe or Cu) coupled by exchange interactions. Each molecule, therefore, presents a mesoscopic system that is neither totally microscopic, nor totally macroscopic, but where micro- and macroscopic behavior coexist. These materials are promising for various practical applications.<sup>2</sup> On the other hand, the coexistence of quantum and classical behavior in the clusters makes them very suitable objects for study of macroscopic quantum effects in spin systems.<sup>3,4</sup> These studies, clarifying many problems of quantum theory of measurements,<sup>5</sup> are also important for development of a physical basis for practical implementation of powerful algorithms of quantum computations, quantum cryptography, and quantum searching.<sup>6</sup>

Particularly, the  $\text{Mn}_{12}\text{O}_{12}(\text{CH}_3\text{COO})_{16}(\text{H}_2\text{O})_4$  molecules (below referred to as  $\text{Mn}_{12}$ ) recently became a subject of great interest. Each molecule<sup>7,8</sup> contains a cluster of twelve manganese ions surrounded by acetate radicals and water molecules. The ground state of the clusters corresponds to a large total spin  $S=10$ . The clusters possess a strong easy-axis anisotropy: the zero-field splitting between the states with  $S_z = \pm 10$  and  $S_z = \pm 9$  (where  $S_z$  is the value of  $z$  projection of the total cluster spin) is 14.4 K. Being stacked into a crystal, the molecules form a tetragonal lattice; in so doing the magnetic interactions between different clusters are very small (of order of  $10^{-2}$  T). Thus, the crystal consisting of these molecules can be considered as an assembly of ideal noninteracting superparamagnetic entities, each being identical to the others.

These clusters have been successfully used for the study of mesoscopic quantum effects. In particular, resonant magnetization tunneling has been unambiguously registered in experiments on  $\text{Mn}_{12}$ .<sup>9,10</sup> There are other experimental results<sup>12,13</sup> supporting the hypothesis of tunneling in  $\text{Mn}_{12}$  below 2 K.

However, the progress in understanding the physical

properties of  $\text{Mn}_{12}$  is greatly hampered by the lack of an adequate description of these clusters. Indeed, the description of  $\text{Mn}_{12}$  as a single spin  $S=10$  entity has been the starting point in most work devoted to this subject. We know of only a few theoretical attempts to account for the internal spin structure of the cluster,<sup>8,14,15</sup> but even in these the relativistic anisotropic interactions have not been taken into account. In view of recent experiments<sup>16-18</sup> showing that the single-spin model is seriously deficient, it is worthwhile reconsidering the many-spin aspects of  $\text{Mn}_{12}$ .

In this paper we focus on the many-spin interactions in  $\text{Mn}_{12}$  clusters. We account for not only isotropic exchange interactions between ions in the cluster, but also various anisotropic interactions possibly present in  $\text{Mn}_{12}$ . Based on the results, we propose a spin Hamiltonian for these clusters. We show that this Hamiltonian can reproduce satisfactorily most recent experimental results, such as positions of neutron scattering peaks, high-frequency EPR data, and the experimental dependence of the magnetic susceptibility on temperature. We note that the account of anisotropic interactions, especially the Dzyaloshinsky-Morya interaction (which has been missing up to now), is crucial for a detailed description of the experimental data.

The paper is organized as follows. In Sec. I we describe the basic model of  $\text{Mn}_{12}$  used in this work and establish roughly its domain of validity. In Sec. II we derive and discuss the spin Hamiltonian for this model. Section III is devoted to discussion of relevant experimental data. In Sec. IV the numerical procedure used for calculations is discussed and the possible parameters of the spin Hamiltonian are presented. Comparison with experimental data is made. The results obtained are analyzed qualitatively and discussed in Sec. V, where the interpretation of the neutron scattering data is presented. A summary is provided in Sec. VI.

## I. THE DIMERIZED 8-SPIN MODEL OF $\text{Mn}_{12}$

The cluster  $\text{Mn}_{12}$ , schematically shown in Fig. 1, consists of eight  $\text{Mn}^{3+}$  ions having the spin 2 and four  $\text{Mn}^{4+}$  ions having the spin 3/2. The ions are coupled by exchange interactions, indicated in Fig. 1 by different lines connecting the

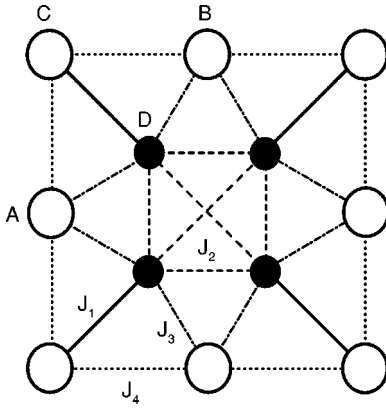


FIG. 1. Schematic plot of the  $\text{Mn}_{12}$  cluster. Small black circles represent  $\text{Mn}^{4+}$  ions; large white circles represent  $\text{Mn}^{3+}$  ions. Different types of lines connecting the ions (solid, dashed, dotted, and dash-dotted) correspond to different types of exchange interactions ( $J_1$ ,  $J_2$ ,  $J_3$ , and  $J_4$ ).

ions. The values of the exchange integrals are not known, but estimates are given in Ref. 8:  $J_1 = -150 \text{ cm}^{-1}$  (AFM exchange),  $J_2 = J_3 = -60 \text{ cm}^{-1}$ , and  $|J_4| < 30 \text{ cm}^{-1}$ . These values are rough, but describe correctly the scale of exchange interactions in  $\text{Mn}_{12}$ . Recent experiments<sup>16–18</sup> show that the excitations with spin values  $S < 10$  are rather close to the ground state: the distance is 40–60 K (values differ in different reports). This is less than the energy of some states with the spin  $S = 10$  (namely, the states  $S_z = 0, \pm 1, \pm 2, \pm 3$ ), i.e., the lower states of the manifold  $S = 9$  are lower than the higher states of the manifold  $S = 10$ . Thus, an adequate description of  $\text{Mn}_{12}$  should account for the excitations with  $S < 10$ ; i.e., the cluster should be considered as a many-spin system.

The total number of spin states in  $\text{Mn}_{12}$  is large even for modern computers. But we can employ the fact that the exchange antiferromagnetic interactions  $J_1$  (see Fig. 1) are much larger than all the others,<sup>8</sup> so corresponding pairs of ions  $\text{Mn}^{3+}$  and  $\text{Mn}^{4+}$  form dimers with the total spin  $s = 1/2$  (one of this pairs is designated in Fig. 1, it includes ions C and D). This model has already been successfully used for description of spin states of the cluster.<sup>8,15</sup> Its validity is proven by megagauss-field experiments:<sup>19</sup> the states of dimers with the spin  $s$  higher than  $1/2$  (excitations of dimers) come into play when the external magnetic field is about 400 T, i.e., the excitations of dimers have energy about  $370 \text{ cm}^{-1}$ . Analogously, the dependence of the magnetic susceptibility of the cluster versus temperature<sup>4,7,8</sup> shows that the dimer excitations contribute when temperature becomes as high as 150–200 K.

Based on these data, we can analyze the domain of validity of the “dimerized” model. To do this, we note that the exchange interactions  $J_2$ ,  $J_3$ , and  $J_4$  mix the ground state of a dimer with the dimer excitations, and the approximation of spin-1/2 dimers corresponds to the zeroth order perturbation theory with  $1/J_1$  as an expansion parameter (similar approach has been used in Ref. 15).

To clarify this point, let us consider the level  $a$  having, to the zeroth order, the energy  $E_a$  with respect to the ground state. Let us denote the distance between the ground state and the excitation of dimer as  $E_{\text{ex}} \sim 370 \text{ cm}^{-1}$ . The first-

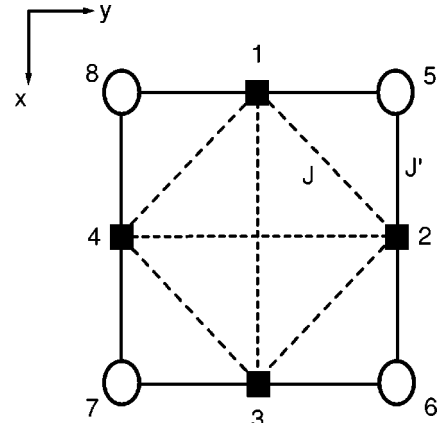


FIG. 2. A schematic plot of the 8-spin system representing the  $\text{Mn}_{12}$  cluster. White large circles represent large spins ( $S = 2$ ), and dark small squares represent small dimer spins ( $s = 1/2$ ).

order correction to the energy of the level  $a$  is of the order of  $J'^2/(E_{\text{ex}} - E_a)$ , where  $J'$  is the magnitude of exchange interactions between dimers and nondimerized spins (see below). Thus, accounting for the first-order corrections, the distance between the ground state and the level  $a$  becomes

$$E'_a = E_a + C_a J'^2 [1/(E_{\text{ex}} - E_a) - 1/E_{\text{ex}}],$$

where  $C_a$  is a factor of order of unity, depending on the specific level  $a$ . As will be shown below,  $J'$  is of order of  $70 \text{ cm}^{-1}$ ; so the first-order correction for the levels with energies about  $70 \text{ cm}^{-1}$  is already considerable, of order of  $4 \text{ cm}^{-1}$ . This estimate, though being rough, gives the correct order of magnitude of the error introduced by the dimerized 8-spin model.

Moreover, this error restricts the region of temperatures where the dimerized model can be successfully applied. For example, as our calculations show, to obtain the correct value of the magnetic susceptibility  $\chi$  at the temperature  $T$ , we need to account for the levels with energies about  $4-5kT$ . Obviously, the error in positions of these levels will introduce corresponding error in the dependence  $\chi(T)$ . Its analytical evaluation is difficult, and the comparison of the results of calculations with the experimental data, performed in Sec. IV is the better way to understand the temperature domain of validity of the dimerized model. As our results show, the dimerized model gives reasonable results for temperatures lower than about 50 K.

Recalling that the temperatures below 30 K are of most interest, we conclude that the dimerized model is satisfactory for present needs of experimentalists.

## II. THE SPIN HAMILTONIAN OF $\text{Mn}_{12}$

Thus, we consider the  $\text{Mn}_{12}$  cluster as consisting of four “small” dimer spins  $s = 1/2$  and four “large” spins  $S = 2$  (corresponding to the four nondimerized ions  $\text{Mn}^{3+}$ ), coupled by exchange interactions (see Fig. 2). Moreover, we

have to account for the anisotropic relativistic interactions in the cluster, so the Hamiltonian of the system can be written as

$$\mathcal{H} = -J \left( \sum_i \mathbf{s}_i \right)^2 - J' \sum_{\langle k,l \rangle} \mathbf{s}_k \mathbf{S}_l + H_{\text{rel}}, \quad (1)$$

where  $\mathbf{s}_i$  are the spin operators of small dimer spins  $s = 1/2$ ,  $\mathbf{S}_l$  are spin operators of large spins  $S = 2$ , and  $H_{\text{rel}}$  denotes the part of the Hamiltonian describing relativistic interactions in the cluster. Summation in Eq. (1) is over pairs of spins coupled by exchange interactions. In the first term of the Hamiltonian we took into account that each small dimer spin is coupled with all the other small spins, so  $2 \sum_i \mathbf{s}_i \mathbf{s}_j = (\sum_i \mathbf{s}_i)^2$  up to an insufficient additive constant.

To zeroth order in  $J_1$ , the exchange integrals of the dimerized models are connected with the initial exchange parameters  $J_2$ ,  $J_3$ , and  $J_4$  as follows:

$$J = -J_2/2, \quad J' = -J_3 + 2J_4. \quad (2)$$

Since the values of  $J_2$ ,  $J_3$ , and  $J_4$  are not known, the parameters  $J$  and  $J'$  are to be determined from experimental data (see Sec. IV).

Furthermore, different types of relativistic anisotropic magnetic interactions possibly present in  $\text{Mn}_{12}$  clusters should be included in the Hamiltonian. A large easy-axis anisotropy in the cluster is one of most important features to be taken into account. Generally, this anisotropy arises due to the single-site anisotropy of large spins (spins of  $\text{Mn}^{3+}$  ions) and various kinds of anisotropic exchange. We performed calculations for three basic types of easy-axis anisotropy in the cluster:

$$H_{\text{rel}}^1 = -K_z \sum_{i=1}^4 (S_i^z)^2, \quad (3a)$$

$$H_{\text{rel}}^2 = -J_{zz} \sum_{\langle i,j \rangle} s_i^z s_j^z, \quad (3b)$$

$$H_{\text{rel}}^3 = -J_{zz} \sum_{\langle i,j \rangle} S_i^z S_j^z, \quad (3c)$$

where summations in Eqs. (3b) and (3c) are over exchange-coupled pairs of spins. Anisotropy parameters ( $K_z$ ,  $J_{zz}$ , or  $J_{zz}$ ) have been chosen to give a correct value of the zero-field splitting between the states  $S_z = \pm 10$  and  $S_z = \pm 9$  (14.4 K). All three types of anisotropy give rather close energies of low-lying excitations (of energy less than 40 K), but higher excitations are reproduced best if the anisotropy is assumed to be of single-site type (3a), so we can conclude that the easy-axis anisotropy is primarily of single-site type. This result agrees with the conclusion drawn in Ref. 21. We will consider only this kind of anisotropy.

Another potentially important sort of relativistic interaction is an in-plane anisotropy of large spins, i.e.,  $H_{\text{rel}}$  can include a contribution of the form:

$$H_{\text{rel}}^4 = K_1 [(S_1^x)^2 + (S_2^y)^2 + (S_3^z)^2 + (S_4^y)^2], \quad (4)$$

where the presence of fourth-order symmetry axis in the cluster is directly taken into account. The small spins  $s$

$= 1/2$  are excluded since  $(\sigma_x)^2 = (\sigma_y)^2 = (\sigma_z)^2 = 1$  for Pauli matrices  $\sigma_x$ ,  $\sigma_y$ , and  $\sigma_z$ ; and only spins of nondimerized  $\text{Mn}^{3+}$  ions give a nontrivial contribution. These ions are surrounded by eight oxygen ions forming a distorted octahedron. The axes of oxygen octahedra are significantly tilted from the  $c$  axis of the cluster, therefore, this term can be relatively large, even comparable to the easy-axis anisotropy. But, surprisingly, our results show that this kind of interaction gives negligible effect, except for trivial renormalization of the easy-axis anisotropy constant  $K_z$  in Eq. (3a). If we account for this renormalization, the positions and the wave functions of excited levels remain almost unaffected even for  $K_1 = 3K_z$  (i.e., for the in-plane anisotropy three times larger than the easy-axis one). Thus, this kind of interaction can be excluded from further considerations.

Another important interaction is Dzyaloshinsky-Morya (DM) antisymmetric exchange. To our knowledge, the possible presence of DM interactions in  $\text{Mn}_{12}$  was first suggested in Ref. 18, but little attention has been paid until now. Our results show that these interactions are, indeed, very important and have rather large magnitude.

A pair of ions coupled by DM interaction is described by the Hamiltonian

$$H_{\text{DM}} = \mathbf{D} \cdot [\mathbf{S}_1 \times \mathbf{S}_2], \quad (5)$$

and the magnitude of the DM vector  $\mathbf{D}$  can be estimated as<sup>22</sup>  $D \sim \lambda A$ , where  $A$  is the isotropic (nonrelativistic) exchange coupling between ions and  $\lambda$  is the spin-orbit coupling constant (which is rather small for transition ions). For comparison, the magnitude of easy-axis anisotropy is estimated as  $K_z \sim \lambda^2 A$ , i.e., is of next order of smallness in comparison with  $D$ . Thus, the DM interactions in  $\text{Mn}_{12}$  can be expected to be important.

In the 8-spin model of the cluster there are DM interactions of two kinds:

$$H_{\text{DM}} = \sum_{\langle i,j \rangle} \mathbf{D}^{i,j} \cdot [\mathbf{s}_i \times \mathbf{S}_j] \quad (6a)$$

$$H_{\text{DM}}^1 = \sum_i \sum_j \mathbf{D}_i^{i,j} \cdot [\mathbf{s}_i \times \mathbf{s}_j]. \quad (6b)$$

Summation in Eq. (6a) is over exchange-coupled pairs of spins; summation in Eq. (6b) is over all pairs of dimer spins, since all dimer spins interact with each other. We studied both kinds of DM interaction and found that the second kind, i.e.,  $H_{\text{DM}}^1$  involving small spins can be neglected. Therefore, we can neglect the interactions of the type (6b).

The crystal field in  $\text{Mn}_{12}$ , governing the DM interactions, possesses certain symmetry elements, thus imposing restrictions on the values of  $\mathbf{D}^{i,j}$ . It is reasonable (and rather standard<sup>22</sup>) to assume that the crystal field is determined mainly by the oxygen octahedra surrounding manganese ions in the cluster; so the symmetry of the crystal field is governed by the mutual arrangement of the oxygen octahedra. The following two symmetry elements are of interest for us. The first one is the fourth-order rotary-reflection axis<sup>7,8</sup> parallel to the  $c$  axis of the cluster. This symmetry is obviously preserved in the 8-spin model of the cluster, so the two DM vectors  $\mathbf{D}^{1,5}$  and  $\mathbf{D}^{1,8}$  (see Fig. 2) define all the other  $\mathbf{D}^{i,j}$ . The other element of symmetry is the mirror plane  $\rho$  parallel

to the  $z$  axis passing through the ions  $C$  and  $D$  (see Fig. 1). The oxygen octahedra surrounding the ions  $A$  and  $B$  (see Fig. 1) are invariant with a good degree of accuracy<sup>20</sup> with respect to reflection in the plane  $\rho$  (inspection of the structure data supplied in Refs. 7 and 8 shows this); this symmetry is also preserved in the 8-spin model. Thus, the vector  $\mathbf{D}^{1,8}$  (Fig. 2) defines all the other DM vectors in the Hamiltonian (6a):

$$D_x^{1,8} = -D_x^{1,5} = D_y^{2,5} = -D_y^{2,6} = -D_x^{3,6} = D_x^{3,7} = -D_y^{4,7} = D_y^{4,8}, \quad (7a)$$

$$D_y^{1,8} = D_y^{1,5} = -D_x^{2,5} = -D_x^{2,6} = -D_y^{3,6} = -D_y^{3,7} = D_x^{4,7} = D_x^{4,8}, \quad (7b)$$

$$D_z^{1,8} = -D_z^{1,5} = D_z^{2,5} = -D_z^{2,6} = D_z^{3,6} = -D_z^{3,7} = D_z^{4,7} = -D_z^{4,8}. \quad (7c)$$

Obviously, any other vector  $\mathbf{D}^{i,j}$  can be taken as a basis instead of  $\mathbf{D}^{1,8}$ . No other symmetry elements allow for further reduction, so DM interactions in  $\text{Mn}_{12}$  are described using three parameters:  $D_x^{1,8}$ ,  $D_y^{1,8}$ , and  $D_z^{1,8}$ . Below, these parameters are denoted simply as  $D_x$ ,  $D_y$ , and  $D_z$ .

As our results show, in the DM Hamiltonian (6a) the terms proportional to  $D_y$  produces negligible matrix elements (a few percent in comparison with other terms). It occurs due to symmetry reasons: the inspection of the relations (7a)–(7c) shows that the components  $D_x$  and  $D_z$  transform antisymmetrically with respect to reflection in the plane  $\rho$ , but the component  $D_y$  transforms symmetrically. The matrix elements of the terms proportional to  $D_y$  nearly cancel each other, leading to negligible matrix elements. Therefore, these terms are excluded from consideration and we set  $D_y = 0$  with negligible error.

Finally, having studied all the interactions described above, we can write down the Hamiltonian of the cluster in the following form:

$$\begin{aligned} \mathcal{H} = & -J \left( \sum_i \mathbf{s}_i \right)^2 - J' \sum_{\langle k,l \rangle} \mathbf{s}_k \mathbf{s}_l - K_z \sum_{i=1}^4 (S_i^z)^2 \\ & + \sum_{\langle i,j \rangle} \mathbf{D}^{i,j} \cdot [\mathbf{s}_i \times \mathbf{s}_j], \end{aligned} \quad (8)$$

where the DM vectors  $\mathbf{D}^{i,j}$  obey the relations (7a)–(7c) with the parameter  $D_y^{1,8} \equiv D_y = 0$ .

### III. REVIEW OF RELEVANT EXPERIMENTAL RESULTS

At present, data of various experiments on magnetic molecules  $\text{Mn}_{12}\text{Ac}$  are available, including the temperature dependence of the effective magnetic moment of the cluster  $\mu_{\text{eff}}(T)$ ,<sup>7,8,16</sup> the results of EPR experiments,<sup>21,23</sup> dynamic susceptibility measurements,<sup>24</sup> inelastic neutron scattering data,<sup>16</sup> and specific heat data.<sup>17</sup> Unfortunately, only few of these data can be used for determining the parameters of the 8-spin Hamiltonian for  $\text{Mn}_{12}$  clusters.

Recent high-frequency EPR experiments<sup>21</sup> refined the description of the easy-axis anisotropy of the cluster and showed that the anisotropy Hamiltonian in the single-spin model can be approximated as follows:

$$H = \alpha S_z^2 + \beta S_z^4 + \gamma(S_+^4 + S_-^4), \quad (9)$$

$$\alpha = -0.56 \text{ K}, \quad \beta = -11.08 \times 10^{-4} \text{ K},$$

$$\gamma = 2.88 \times 10^{-5} \text{ K},$$

where  $S_z$ ,  $S_+$ , and  $S_-$  denote the operators of the total spin of the cluster. It means, in terms of a many-spin approach, that the energies of the low-lying levels with spin  $S=10$  obey Eq. (9). It is worth noting that the derived values of quartic corrections  $\beta$  and  $\gamma$  are rather large and, as our calculations show (see below), seem to be poorly explained using the single-spin description of  $\text{Mn}_{12}$ , i.e., when accounting only for the states belonging to the  $S=10$  manifold. Our results show that the excited levels with  $S < 10$  are necessary to give reasonable values for the quartic corrections.

Another set of results, very useful for elucidating the many-spin interactions in  $\text{Mn}_{12}\text{Ac}$ , is the neutron scattering results supplied in Ref. 16. The experiments have been performed at very low temperatures (mostly, 1.5 K to 2.5 K), where only the lowest levels  $S_z = \pm 10$  are populated. Since the selection rule for neutron scattering is  $\delta S_z = 0, \pm 1$ , only the levels with  $S_z = \pm 9$  can give rise to scattering peaks (the levels with  $S_z = \pm 11$  have too large energies<sup>19</sup> and can be excluded).

Results of these experiments can be summarized as follows. A prominent peak of spin origin at about 0.3 THz has been detected and attributed to the transitions to the levels with  $S=10, S_z = \pm 9$ , in excellent agreement with all previous data (0.3 THz corresponds to about 14.4 K). At higher energies, two sets of peaks have been detected around 1.2 THz and 2.0 THz. The fitting proposed in Ref. 16 gives two peaks in the first set (at energies about 57 K and 66 K) and three peaks in the second set (at energies 90 K, 96 K, and 105 K); but authors indicate clearly that possibly more peaks are present (most likely, three peaks in the first set and four or five in the second). Another interesting detail of the neutron scattering spectra is a very broad mode situated at about 0.2 THz; this mode disappears when the temperature is less than about 2 K.

The authors have not managed to interpret these features, except for the peak at 0.3 THz. They pointed out that there is particular difficulty in interpretation of the peaks at 1.2–1.3 THz: the model they used for susceptibility fitting gives two degenerate levels  $S=9$  at about 33 K, an obvious contradiction with the neutron scattering spectrum. We show below that the 8-spin model developed here can overcome these difficulties and gives correct positions for neutrons peaks at 1.2 THz along with a correct description of the susceptibility data.

Thus, we found the following experimental results to be relevant for the purpose of a quantitative description of the  $\text{Mn}_{12}$  clusters. The distance between the ground state and the first excited level(s) is 14.4 K. The energies (the anisotropy splittings) of the low-lying levels, belonging to the  $S=10$  manifold, obey formula (9). There are two or three neutron peaks around 60–70 K, two of them are situated at 57 K and 66 K. Also, there are up to five peaks around 100 K, three of them are at 90 K, 96 K, and 105 K. The temperature depen-

dence of the susceptibility [or, equivalently, the dependence  $\mu_{\text{eff}}(T)$ ] has the form displayed in Refs. 7, 8, and 16 and Fig. 4.

The other experimental results, though providing important information about  $\text{Mn}_{12}$ , are much less suitable for our purposes (to a large extent, because different, *a priori* equally probable, interpretations are possible).

#### IV. NUMERICAL CALCULATIONS AND PARAMETERS OF THE 8-SPIN MODEL. COMPARISON WITH EXPERIMENT

Having derived the spin Hamiltonian for the 8-spin model of  $\text{Mn}_{12}$ , we attempted to extract its parameters from the relevant experimental data.

We used the following two-step numerical scheme. At the first step, the relativistic term  $H_{\text{rel}}$  has been neglected resulting in an isotropic exchange Hamiltonian. The eigenstates of this Hamiltonian are degenerate with respect to  $S_z$ . Thus, it is sufficient to take into account only the states with  $S_z=0$ , so the exchange Hamiltonian (represented by a matrix  $1286 \times 1286$ ) has been diagonalized within the subspace spanned by these states. Then, at the second step, the relativistic anisotropic interactions have been taken into account. Among the states obtained at the first step (having  $S_z=0$ ), we retain only those with the energy less than  $E_{\text{cut}}$  (a sufficiently large value for this parameter has been chosen) and generate the corresponding states with different  $S_z$  (basis states). Then the complete Hamiltonian (8) has been diagonalized within the subspace spanned by the generated basis states. Calculations with different values of  $E_{\text{cut}}$  have been performed to assure that the positions of lower levels are obtained with desired accuracy. Typical values of  $E_{\text{cut}}$  were about 250 K: the levels with higher energies are not worth including due to the limited accuracy of the 8-model itself (see Sec. I).

Based on the procedure described above, the fitting of relevant experimental data (Sec. III) has been made and the possible parameters of the 8-spin Hamiltonian determined.

Neutron scattering data are of primary interest for us. We focus our attention on the positions of the neutron peaks, since the amplitudes depend strongly on details of the experiments. We first assume an ideal experiment, where the resolution of the setup is infinite and the neutrons with all possible scattering vectors are detected (i.e., the detector has infinite aperture). In this case, at zero temperature, the cross section of neutron scattering at the energy  $E$  is<sup>16,25</sup>

$$\begin{aligned} \sigma(E) = & \int_{\mathbf{R}^3} d^3\mathbf{q} A F^2(q) \sum_{a,b} (\delta_{a,b} - q_a q_b / q^2) \\ & \times \sum_{m,n} \exp[i\mathbf{q}(\mathbf{r}_m - \mathbf{r}_n)] \\ & \times \sum_{\psi} \langle 0 | S_m^a | \psi \rangle \langle \psi | S_n^b | 0 \rangle \delta(E(\psi) - E), \quad (10) \end{aligned}$$

where  $A$  is a constant,  $F(q)$  is the form factor of manganese ions,  $\mathbf{q}$  is a scattering vector,  $n, m$  enumerate different ions, and  $a, b$  refer to the Cartesian coordinates ( $x$ ,  $y$ , and  $z$ ). The integration is performed over all vectors  $\mathbf{q}$ .  $E(\psi)$  denotes the energy of the state  $\psi$ ,  $|0\rangle$  denotes the ground state, which is the only one populated at zero temperature. The

transitions with  $\Delta S_z = 0, +1$  can be neglected since there is only one state  $S_z = 10$  and no states  $S_z = 11$ . In this case, the total cross section (10) is proportional to the quantity

$$V = \sum_i |\langle \phi_i^{(9)} | \psi \rangle|^2, \quad (11)$$

where the state  $\psi$  has the energy  $E(\psi) = E$  with respect to the ground state; i.e., the state  $\psi$  is the final state of the neutron scattering process and gives rise to a neutron peak at the energy  $E(\psi)$  of the amplitude proportional to  $V$ . The summation in Eq. (11) is performed over all basis levels having  $S_z = 9$ ; these levels are denoted as  $\phi_i^{(9)}$ . Equation (11) expresses the simple fact that only the transitions with  $\Delta S_z = -1$  are allowed in the neutron scattering process, since the transitions with  $\Delta S_z = 0, +1$  are absent. Below, the quantity  $V$  is referred to as a normalized cross section for the level  $\psi$ . Our results show that  $V$  discriminates easily the eigenstates which can give rise to noticeable neutron scattering peaks.

Furthermore, the values of parameters  $\alpha$  and  $\beta$  describing the easy-axis anisotropy in Eq. (9), have been taken into account in determination of the cluster parameters. The energies of the five lowest levels, having spin  $S = 10$ , have been approximated by a fourth-order polynomial, following Eq. (9), and the coefficients  $\alpha$  and  $\beta$  have been extracted and compared to the experimental data.

As a result of calculations, the following three sets of the cluster parameters have been found to provide the best fitting of experimental data:

Set A:

$$J=0, \quad J'=105 \text{ K}, \quad K_z=5.69 \text{ K}, \\ D_z=-1.2 \text{ K}, \quad D_x=25 \text{ K};$$

Set B:

$$J=23.8 \text{ K}, \quad J'=79.2 \text{ K}, \quad K_z=5.72 \text{ K}, \\ D_z=10 \text{ K}, \quad D_x=22 \text{ K};$$

Set C:

$$J=41.4 \text{ K}, \quad J'=69 \text{ K}, \quad K_z=5.75 \text{ K}, \\ D_z=10 \text{ K}, \quad D_x=20 \text{ K}.$$

The positions of neutron peaks calculated for these sets of parameters are presented in Fig. 3. The graphs show the dependence of normalized cross section versus the level energy. It is seen from these figures, that the normalized cross section is extremely small (less than  $10^{-2}$ ) for most of levels, and only few states can give rise to noticeable neutron scattering peaks. Moreover, to facilitate the analysis of the data for the reader, the positions of neutron peaks are listed in the Table I. The values of the easy-axis anisotropy parameters  $\alpha$  and  $\beta$  are listed in the Table II.

As the results show, each of the parameter sets reproduces reasonably well its own portion of the experimental results. All the sets give reasonably good positions of the low-energy neutron peaks at 0.3 THz (14.4 K), 1.19 THz (57 K), and 1.38 THz (66 K). The parameter set A also gives the values of anisotropy parameters  $\alpha$  and  $\beta$ , rather close to the experimental ones, but the neutron peaks corresponding to higher energies (around 2 THz) are reproduced poorly. The param-

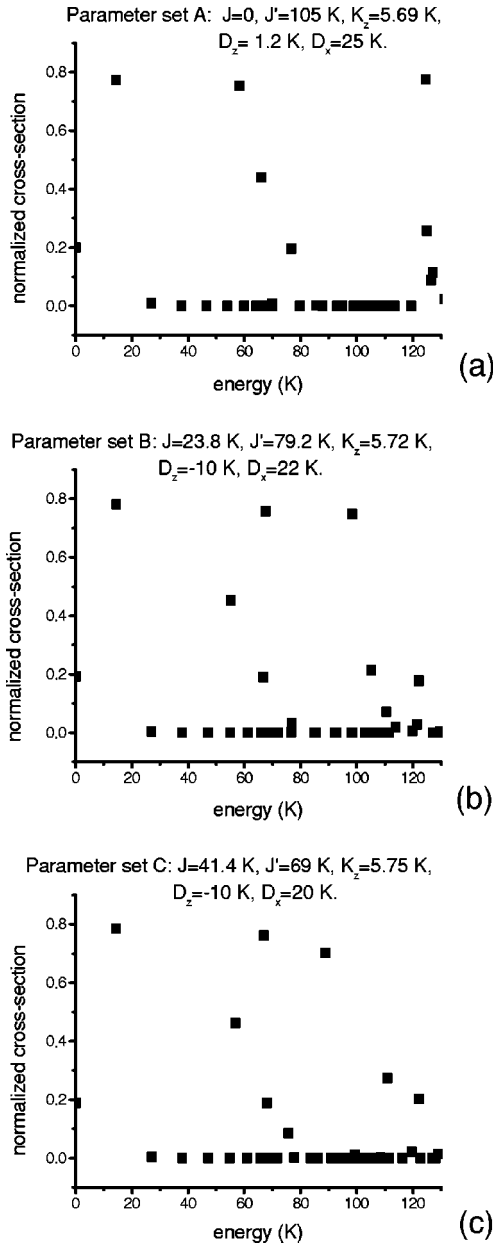


FIG. 3. Dependence of the normalized cross section vs level energy (in K), calculated for the three sets of the cluster parameters (A, B, and C; see text). The levels producing noticeable neutron peaks can be easily discriminated from the others.

eter sets B and C give correctly only the order of magnitude of  $\alpha$  and  $\beta$ , but reproduce better the positions of the high-energy neutron peaks.

Finally, the temperature dependence of the effective magnetic moment  $\mu_{\text{eff}}$  of the cluster has been calculated for all three sets of parameters using the formula

$$\mu_{\text{eff}}(T) \equiv \sqrt{3\chi(T) \cdot kT}, \quad (12)$$

where  $\chi$  is the susceptibility of the cluster,  $k$  is Boltzmann's constant, and  $T$  is the temperature. The susceptibility  $\chi(T)$  has been calculated in a way reproducing the experimental procedure. The Zeeman term, describing the effect of an external field has been introduced into the Hamiltonian (8). The

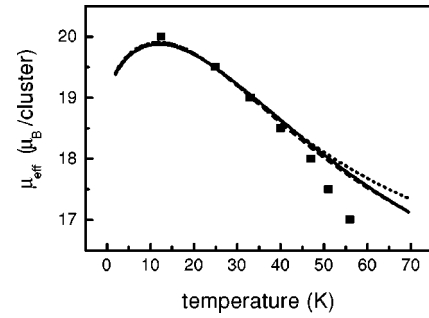


FIG. 4. Temperature dependence of the effective magnetic moment of the cluster  $\mu_{\text{eff}}$  (in Bohr's magnetons). Results of calculations with the three sets of parameters are shown: the set A (solid line), the set B (dashed line), and the set C (dotted line). Large solid squares represent experimental data. The results of calculations with the sets A and B are very close to each other, and the corresponding curves merge on the figure.

field magnitude  $H = 1$  mT has been chosen following Ref. 16. The resulting Hamiltonian has been diagonalized, and the component of the cluster spin  $S_H$  along the field has been calculated by means of quantum-statistical averaging over the Gibbs canonical ensemble. This routine has been repeated several times for different orientations of the field, and the obtained values of  $S_H$  have been averaged. It corresponds to powder sample measurements, when the crystallites are randomly oriented with respect to the field. The susceptibility  $\chi$ , following a standard experimental procedure, has been calculated as a ratio of the resulting average cluster spin to the field magnitude  $H$ . Finally, the value  $\mu_{\text{eff}}$  has been obtained applying Eq. (12).

The curves  $\mu_{\text{eff}}$  calculated for the three sets of cluster parameters, are presented in Fig. 4 along with the experimental data. All the sets give almost coinciding curves, and below 50 K the agreement with experiment is good. The region of temperatures higher than 50 K cannot be reproduced satisfactorily: as our test calculations showed, to obtain the correct value of effective moment  $\mu_{\text{eff}}$  at the temperature  $T$ , we need to account for the levels with energies about  $4-5kT$ . When calculating the curves presented, only the levels with energies less than 250 K have been taken into account, thus restricting the correctly described temperature region.

## V. QUALITATIVE ANALYSIS OF THE RESULTS AND INTERPRETATION OF EXPERIMENTAL DATA

At present, having rather limited number of the relevant experimental data, it is hard to distinguish between the parameter sets A, B, and C. The easy-axis anisotropy parameters  $\alpha$  and  $\beta$  are obtained with good precision in EPR experiments, but the magnetization measurement data<sup>18</sup> suggest other values for these parameters; so, comparison of the experimental values of  $\alpha$  and  $\beta$  with our results cannot serve as a definitive basis for judgement. Also, the quality of the description of the high-energy neutron peaks cannot be decisive, since the disagreement can be attributed to the limited accuracy of the dimerized 8-spin model itself. Megagauss-field experiments,<sup>19</sup> along with careful measurements of the low-energy peaks (around 1.2 THz) and fitting of their am-

TABLE I. The positions of neutron peaks: comparison between experimental data and calculated results. Calculations have been made for the three possible sets of the cluster parameters (A, B, and C; see text). The levels with normalized cross section more than 0.05 and energy less than 130 K are included in the table.

	Experiment	Set A	Set B	Set C
	14.4 K	14.4 K	14.4 K	14.4 K
Low-energy peaks (1.2 THz)	57 K	58.2 K	55.2 K	56.7 K
	66 K	66.0 K	66.7 K	67.0 K
	maybe,		67.4 K	67.9 K
	more	76.6 K		75.7 K
High-energy peaks (2 THz)	90 K	124.4 K	98.3 K	88.8 K
	96 K	124.9 K	105.1 K	110.9 K
	105 K	126.4 K	110.4 K	122.1 K
	maybe,	127.1 K	122.1 K	
	more			

plitudes seems to be a promising strategy for future investigations.

Nevertheless, the results already obtained provide new important information about the role of many-spin interactions in  $\text{Mn}_{12}$  clusters. In this section we focus our attention on the qualitative consideration of the results obtained and discuss the interpretation of the experimental data.

First, it is worthwhile to note that the consideration of states with spin  $S$  less than 10 leads to rather large quartic corrections to the energy of easy-axis anisotropy. If these excited states are not taken into account, i.e., if only the states with  $S=10$  are included, the value of  $\beta$  is of order of  $10^{-5}$  K.

Another important fact is the large magnitude of the Dzyaloshinski-Morya (DM) interactions in the cluster  $\text{Mn}_{12}$ . In our opinion, this can be attributed to the low symmetry of the cluster. Indeed, the strength of the DM interaction is governed to a large extent by asymmetry of crystal field acting on the interacting ions.<sup>22</sup> An instructive example is provided in Ref. 26: the DM interaction can emerge for ions located at the surface of a magnet, even though these interactions are prohibited for ions in the bulk of the magnet. In some sense the  $\text{Mn}_{12}$  molecule possesses “surface” everywhere, and the symmetry of the crystal field is rather low.

The presence of the large Dzyaloshinsky-Morya term in the Hamiltonian provides a key to an explanation of the neutron scattering data. First, the DM terms lead to the appearance of the two neutron peaks around 1.2 THz. If these terms are absent, there are two degenerate levels with  $S_z=9$

TABLE II. Parameters  $\alpha$  and  $\beta$  of the easy-axis anisotropy: comparison between experimental data and calculated results. Calculations have been performed for the three possible sets of the cluster parameters (A, B, and C; see text).

	Experiment	Set A	Set B	Set C
$\alpha$ (K)	-0.56	-0.63	-0.68	-0.67
$\beta$ (mK)	-1.11	-0.7	-0.45	-0.49

around 1.2 THz. Among all the interactions we considered (see Sec. II), only the DM interaction can lift this degeneracy and provide a large splitting (about 9 K), as observed in experiments. Similarly, according to our calculations, several peaks around 2 THz appear only due to DM interactions.

The origin of the peak at 0.3 THz has been completely explained in Ref. 16: it appears because of easy-axis anisotropy splitting the levels with different  $S_z$ . Our results agree with this conclusion.

An interesting feature in the neutron scattering data is the broad mode situated at 0.2 THz. No states of this energy have been observed, e.g., in EPR experiments.<sup>8,21,23</sup> Our calculations also show no states with the energy 0.2 THz (or, equivalently, about 10 K). In our opinion, this mode is caused by an interaction of  $\text{Mn}_{12}$  clusters with the dissipative environment. Due to this interaction, each level broadens (nonuniform broadening), forming a quasiband of finite width  $\delta E$  (see Refs. 11, 27 for details). The value of  $\delta E \approx 2$  K can be estimated from the single-crystal hysteresis measurements.<sup>10</sup> Transitions between the two quasibands take place, so, along with the peak at 0.3 THz (14.4 K), a broad mode of interquasiband transitions appears. It happens when different states in the quasibands are populated, i.e., at the temperatures of order of  $\delta E \approx 2$  K, which agrees with experiment. Energies of the interquasiband transitions are reduced by the value about  $2 \cdot \delta E \approx 4$  K, so the corresponding neutron scattering mode is situated around  $E_b = 14.4 \text{ K} - 2 \cdot \delta E \approx 10.4 \text{ K}$ , or, equivalently, around 0.2 THz, in agreement with experiment. At increasing temperatures, the occupancy of quasibands becomes more uniform, so the intensity of the broad mode increases along with the decrease in intensity of the peak at 14.4 K. This behavior also agrees with experiment. However, this qualitative explanation cannot be considered as sufficient, and a rigorous quantitative treatment is necessary. Such a treatment constitutes a separate physical problem to be investigated in the future.

## VI. SUMMARY

In the present work, we have performed an extensive study of spin excitations in  $\text{Mn}_{12}$ , explicitly accounting for its many-spin internal structure. The dimerized 8-spin model of the  $\text{Mn}_{12}$  clusters<sup>8</sup> has been used. Along with isotropic exchange coupling, various kinds of anisotropic relativistic interactions have been studied: anisotropic exchange coupling between the cluster ions, single-site anisotropies of easy-axis and in-plane type, and various kinds of Dzyaloshinsky-Morya (DM) interactions. Surprisingly, most of these interactions play only a minor role.

As a result, we propose a basic many-spin Hamiltonian which includes isotropic exchange couplings, single-site anisotropies of easy-axis type, and DM interactions between the cluster spins. Three possible sets of parameters are determined from the relevant experimental data. The results of our calculations reproduce satisfactorily various experimental results, such as positions of neutron scattering peaks, high-frequency EPR data, and the experimental dependence of the magnetic susceptibility on temperature. In particular, our results suggest rather strong Dzyaloshinsky-Morya interactions are present in the  $\text{Mn}_{12}$  cluster.

## ACKNOWLEDGMENTS

The authors would like to thank A. K. Zvezdin, B. Barbara, and D. Garanin for many helpful discussions. This work was partially carried out at the Ames Laboratory, which is operated for the U.S. Department of

Energy by Iowa State University under Contract No. W-7405-82 and was supported by the Director for Energy Research, Office of Basic Energy Sciences of the U.S. Department of Energy. This work was partially supported by Russian Foundation for Basic Research, Grant No. 98-02-16219.

- <sup>1</sup>O. Kahn, *Molecular Magnetism* (VCH, New York, 1993); D. Gatteschi, A. Caneschi, L. Pardi, and R. Sessoli, *Science* **265**, 1054 (1994).
- <sup>2</sup>*Molecular Magnetism: From Molecular Assemblies to the Devices*, edited by E. Coronado, P. Delhaès, D. Gatteschi, and J.S. Miller (Kluwer, Dordrecht, 1996).
- <sup>3</sup>A.J. Leggett, *Prog. Theor. Phys. Suppl.* **69**, 80 (1980).
- <sup>4</sup>*Quantum Tunneling of Magnetization — QTM'94*, Vol. 301 of *NATO Advanced Study Institute, Series E*, edited by L. Gunther and B. Barbara (Kluwer, Dordrecht, 1995).
- <sup>5</sup>M.B. Menskii, *Continuous Quantum Measurements and Path Integrals* (IOP Publishing, Bristol, 1993).
- <sup>6</sup>P.W. Shor, *SIAM J. Comput.* **26**, 1484 (1997); N. Gershenfeld and I.L. Chuang, *Science* **275**, 350 (1997).
- <sup>7</sup>T. Lis, *Acta Crystallogr., Sect. B: Struct. Crystallogr. Cryst. Chem.* **B36**, 2042 (1980); R. Sessoli, D. Gatteschi, A. Caneschi, and M.A. Novak, *Nature (London)* **365**, 141 (1993).
- <sup>8</sup>R. Sessoli, H.-L. Tsai, A.R. Shake, S. Wang, J.B. Vincent, K. Folting, D. Gatteschi, G. Christou, and D.N. Hendrickson, *J. Am. Chem. Soc.* **115**, 1804 (1993).
- <sup>9</sup>J.R. Friedman, M.P. Sarachik, J. Tejada, and R. Ziolo, *Phys. Rev. Lett.* **76**, 3830 (1996).
- <sup>10</sup>L. Thomas, F. Lioni, R. Ballou, D. Gatteschi, R. Sessoli, and B. Barbara, *Nature (London)* **383**, 145 (1996).
- <sup>11</sup>F. Hartmann-Boutron, P. Politi, and J. Villain, *Int. J. Mod. Phys. B* **10**, 2577 (1996).
- <sup>12</sup>B. Barbara, W. Wernsdorfer, L.C. Sampaio, J.G. Park, C. Paulsen, M.A. Novak, R. Ferré, D. Mailly, R. Sessoli, A. Caneschi, K. Hasselbach, A. Benoit, and L. Thomas, *J. Magn. Magn. Mater.* **140-144**, 1825 (1995).
- <sup>13</sup>C. Paulsen and G. Park, in *Quantum Tunneling of Magnetization* (Ref. 4), p. 189.
- <sup>14</sup>A. Caneschi, D. Gatteschi, L. Pardi, and R. Sessoli, in *Perspectives on Coordination Chemistry*, edited by A.F. Williams, C. Florani, and A.E. Merbach (VCH, Basel, 1992).
- <sup>15</sup>A.K. Zvezdin and A.I. Popov, *Sov. Phys. JETP* **82**, 1140 (1996).
- <sup>16</sup>M. Hennion, L. Pardi, I. Mirebeau, E. Suard, R. Sessoli, and D. Gatteschi, *Phys. Rev. B* **56**, 8819 (1997).
- <sup>17</sup>A.M. Gomes, M.A. Novak, R. Sessoli, A. Caneschi, and D. Gatteschi, *Phys. Rev. B* **57**, 5021 (1998).
- <sup>18</sup>B. Barbara, L. Thomas, F. Lioni, A. Sulpice, and A. Caneschi, *J. Magn. Magn. Mater.* **177-181**, 1324 (1998).
- <sup>19</sup>A.A. Mukhin, A.K. Zvezdin, V.V. Platonov, O.M. Tatsenko, A. Caneschi, D. Gatteschi, and B. Barbara, in *Proceedings of ICM'97 Conference*, Cairns, Australia, 1997 (unpublished).
- <sup>20</sup>Although this symmetry is not exact, the deviation from the symmetry is small. Such approximate symmetries are widely used in physics: e.g., the crystal lattice of ferromagnetic iron is often considered as cubic, though actually it is tetragonally distorted.
- <sup>21</sup>A.L. Barra, D. Gatteschi, and R. Sessoli, *Phys. Rev. B* **56**, 8192 (1997).
- <sup>22</sup>K. Yosida, *Theory of Magnetism* (Springer-Verlag, Berlin, New York, 1996).
- <sup>23</sup>S. Hill, J.A.A.J. Perenboom, N.S. Dalal, T. Hathaway, T. Stalcup, and J.S. Brooks, *Phys. Rev. Lett.* **80**, 2453 (1998).
- <sup>24</sup>F. Luis, J. Bartolomé, J.F. Fernández, J. Tejada, J.M. Hernández, X.X. Zhang, and R. Ziolo, *Phys. Rev. B* **55**, 11 448 (1997).
- <sup>25</sup>See, e.g., R.M. White, *Quantum Theory of Magnetism* (Springer-Verlag, Berlin, New York, 1983).
- <sup>26</sup>A. Crépieux and C. Lacroix, *J. Magn. Magn. Mater.* **182**, 341 (1998).
- <sup>27</sup>V.V. Dobrovitski and A.K. Zvezdin, *Europhys. Lett.* **38**, 377 (1997); L. Gunther, *ibid.* **39**, 1 (1997).